

Role of dissipation on the quasielastic barrier distributions: The case of $^{20}\text{Ne} + ^{92,94,95}\text{Mo}$ systems

G. COLUCCI⁽¹⁾, A. TRZCIŃSKA⁽¹⁾, E. PIASECKI⁽¹⁾, M. WOLIŃSKA-CICHOCA⁽¹⁾,
A. BARBON⁽²⁾⁽³⁾, G. D'AGATA⁽²⁾, E. DE FILIPPO⁽²⁾, Z. K. CZERSKI⁽⁴⁾,
R. DUBEY⁽⁴⁾, E. GERACI⁽²⁾⁽³⁾, B. GNOFFO⁽²⁾, K. HADYŃSKA-KŁĘK⁽¹⁾,
G. JAWORSKI⁽¹⁾, M. KISIELIŃSKI⁽¹⁾, P. KOCZOŃ⁽⁵⁾, M. KONDZIELSKA⁽⁶⁾,
M. KOWALCZYK⁽¹⁾, Y. LEIFELS⁽⁵⁾, B. LOMMEL⁽⁵⁾, M. MATUSZEWSKI⁽¹⁾,
N. S. MARTORANA⁽²⁾, E. V. PAGANO⁽⁷⁾, L. QUATTROCCHI⁽²⁾, F. RISITANO⁽²⁾,
P. RUSSOTTO⁽⁷⁾, J. SAMORAJCZYK-PYŚK⁽¹⁾, A. STOLARZ⁽¹⁾, G. TIURIN⁽⁸⁾,
M. TRIMARCHI⁽¹⁾, W. H. TRZASKA⁽⁸⁾, A. TUCHOLSKI⁽¹⁾, C. ZAGAMI⁽³⁾⁽⁷⁾
and B. ZALEWSKI⁽¹⁾

⁽¹⁾ Heavy Ion Laboratory, University of Warsaw - Warsaw, Poland

⁽²⁾ INFN, Sezione di Catania - Catania, Italy

⁽³⁾ Dipartimento di Fisica e Astronomia, University of Catania - Catania, Italy

⁽⁴⁾ Institute of Physics, University of Szczecin - Szczecin, Poland

⁽⁵⁾ GSI Helmholtzzentrum für Schwerionenforschung GmbH - Darmstadt, Germany

⁽⁶⁾ Faculty of Physics, University of Warsaw - Warsaw, Poland

⁽⁷⁾ INFN-LNS, Laboratori Nazionali del Sud - Catania, Italy

⁽⁸⁾ University of Jyväskylä - Jyväskylä, Finland

received 26 November 2024

Summary. — The quasielastic barrier distributions of the $^{20}\text{Ne} + ^{92,94,95}\text{Mo}$ systems were measured at the Heavy Ion Laboratory (HIL) of the University of Warsaw. The preliminary results provide evidence of the influence of dissipation due to single-particle excitations on the structure of the barrier distribution. The increasing number of single-particle excitations for the heaviest Mo isotopes smoothes out the barrier distribution, which loses the structure predicted by the coupling to only collective excitations. Theoretical calculations which include the coupling to the non-collective excitation agree with the experimental data. The measurement of the differential transfer cross-sections of the three systems should clarify the role that the dissipation due to transfer might play on the smearing of the barrier distribution.

1. – Introduction

One of the most interesting near-Coulomb barrier reactions is fusion. It is well known that there is a connection between this reaction mechanism and the internal degrees of freedom of the interacting nuclei, which manifests itself as a strong enhancement of the fusion cross-section at sub-barrier energies in comparison with the simple model of the Coulomb barrier transmission. In the frame of the Coupled Channels (CC) model [1,2], this is interpreted as a result of the couplings between the relative motion and nuclear

intrinsic degrees of freedom, such as collective inelastic excitations of the colliding nuclei. Following the couplings, the single Coulomb barrier is replaced by several barriers, one for each coupling channel, and their weighted sum generates the barrier distribution. Consequently, the barrier distributions tend to present significant differences among different systems, giving a fingerprint of the dynamics of the reaction [3].

The CC model succeeded in reproducing the experimental excitation functions as well as the observed structures in the barrier distributions for many systems. However, there are several mechanisms still not clear. Among these, the influence of weak reaction channels, such as non-collective excitations and transfer, stands out.

The experimental quasielastic barrier distributions (D_{qe}) of some systems turned out to be structureless, in contradiction with the theoretical predictions. This was observed in the case of the $^{20}\text{Ne} + ^{90,92}\text{Zr}$ systems [4,5]. The CC calculations predicted for the two systems very similar two-peak structured barrier distributions because of the strongly deformed ^{20}Ne and the dominant role that its rotational excitations play in the coupling with respect to the vibrational excitations of Zr isotopes. Contrarily to the predictions, the experimental D_{qe} of the $^{20}\text{Ne} + ^{92}\text{Zr}$ showed a significantly smoother structure than the one observed for the $^{20}\text{Ne} + ^{90}\text{Zr}$. The cause of the different structures in the barrier distributions was found in a dissipative mechanism, where part of the kinetic energy is dissipated into the excitation of single-particle (s.p.) levels. Although the coupling to the non-collective excitation is usually negligible, if the density of s.p. levels is significantly high, the coupling to these levels can influence the reaction, and thus, the shape of the barrier distribution. This is the case of the ^{92}Zr , where the two neutrons outside the $N = 50$ closed shell lead to a higher s.p. level density than of the ^{90}Zr .

Similar studies performed for the $^{20}\text{Ne} + ^{58,60,61}\text{Ni}$ [6] and $^{24}\text{Mg} + ^{90,92}\text{Zr}$ [7] confirmed the hypothesis and triggered the development of a new model able to include the non-collective excitations. The new method, named CCRMT, merges a statistical approach with quantum mechanics by extending the CC method using the random matrix theory (RMT) [8]. The CCRMT calculations were applied to the $^{20}\text{Ne} + ^{90,92}\text{Zr}$ [9], where the couplings to many non-collective levels smoothed the peak structure of the barrier distribution in the $^{20}\text{Ne} + ^{92}\text{Zr}$ system, while only slightly influencing it for the $^{20}\text{Ne} + ^{90}\text{Zr}$. An analogous agreement was obtained for the Ni isotopes, especially for the ^{61}Ni .

Recently at the Heavy Ion Laboratory (HIL) of the University of Warsaw, the quasielastic barrier distributions of $^{20}\text{Ne} + ^{92,94,95}\text{Mo}$ systems were measured [10]. The experiment aimed at studying the influence of dissipation due to non-collective excitations on the shape of the barrier distributions. In this perspective, the strongly deformed ^{20}Ne was chosen as the projectile, while isotopes of the same element, which differ by single-particle level densities and with relatively weak collective excitations, were used as target nuclei. The density of the single-particle levels gradually increases with the atomic masses of the three isotopes, thus a smoothing of the barrier distributions should manifest in the heavier Mo isotopes.

2. – Quasielastic barrier distribution

At HIL, the U200-P Cyclotron provided the ^{20}Ne beam at an average current of 25 enA and energies of 65, 70 and 73 MeV, while ~ 0.5 MeV energy steps measurements were performed by using as degraders thin ^{nat}Ni and ^{nat}Au foils. Thin MoO_3 targets on a C backing of $40 \mu\text{g}/\text{cm}^2$ thickness were used. The ^{92}Mo (enriched to 98.27%), ^{94}Mo (92.03%) and ^{95}Mo (96.47%) targets had a thickness of 181, 156 and $162 \mu\text{g}/\text{cm}^2$, respectively.

The compact CUDAC3 chamber was employed. The setup allowed us to measure the quasielastic barrier distribution with the back-scattering method: an array of 30 silicon detectors (PIN diodes) placed at the backward angles of 145, 135, and 125 degrees provided the energy and number of the backscattered projectiles, while four detectors at the forward angle of 35 degrees were used for normalization by Rutherford scattering. The forward detectors also constantly monitored the beam energy and its resolution, which was determined mainly by the beam properties and equal to ~ 1.5 MeV, 2.2 MeV and 1.3 MeV (in the center-of-mass system) for $^{92,94,95}\text{Mo}$, respectively.

The cross-sections for quasielastic scattering σ_{qe} and Rutherford scattering σ_{Ruth} values for each measured energy were estimated by converting the energy spectra of the detected ions into Q -value spectra and then by integrating them in the range of -5 MeV and 11 MeV. Subsequently, the data were binned in 0.5 MeV intervals and the $\sigma_{qe}/\sigma_{Ruth}$ ratios were normalized to the lowest energy measured ones. In this way, precise information on detectors' solid angles, target thickness and absolute beam current, as well as associated systematic errors, could be neglected.

The quasielastic barrier distributions were extracted from the excitation function using the finite-difference method [3,4]. The preliminary experimental results are compared with theoretical calculations in fig. 1. The theoretical calculations were performed within the CC method (dashed lines) by including the rotational coupling to the first three excited states of ^{20}Ne and vibrational couplings up to the two-phonons excitations of the first quadrupole and octupole excited states of $^{92,94}\text{Mo}$ isotopes. In the case of the ^{95}Mo isotope, the couplings to the one phonon excitation of the $3/2^+$ and the two phonons excitations of the $5/2^+$ excited states were included.

The experimentally determined D_{qe} is still structured for the ^{92}Mo target, where the level density is low, as foreseen by the CC model. On the other hand, such structure is significantly smoothed out for the ^{94}Mo and ^{95}Mo targets, which present a higher s.p. level density.

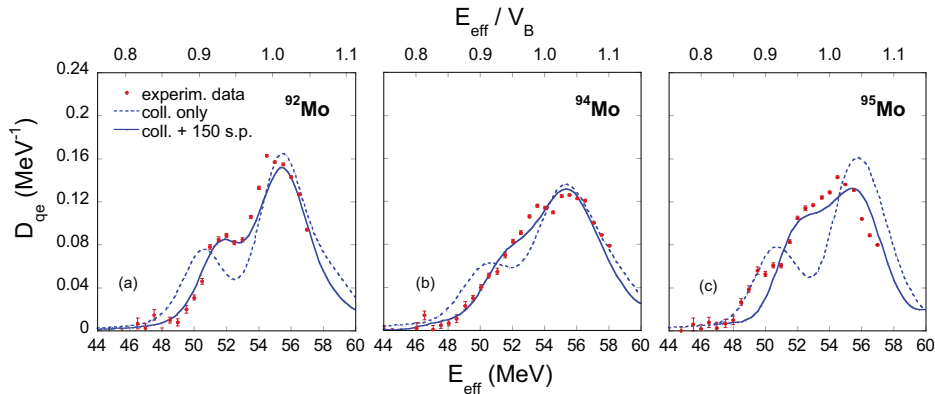


Fig. 1. – Comparison of the preliminary experimental barrier distributions of the $^{20}\text{Ne} + ^{92,94,95}\text{Mo}$ systems with the theoretical predictions. The calculations obtained including (solid blue lines) and not including (dashed blue lines) dissipation due to non-collective excitations are shown. On the top axis, the energy scale is normalized to the height of the Coulomb barriers V_B estimated according to Akyüz-Winther parametrization. The energy resolutions for the three systems were taken into account.

The couplings to the first 150 s.p. levels of the target nuclei were included (solid lines) within the CCRMT model. When the couplings to the non-collective excitations are taken into account, the calculations nicely reproduce the experimental D_{qe} of the $^{20}\text{Ne}+^{92,94,95}\text{Mo}$ systems. However, in the intermediate case of the ^{94}Mo isotope, the structure of the experimental barrier distribution is smoother and wider with respect to the one of ^{95}Mo , although it has a higher level density.

3. – Differential transfer cross-section

The effect of couplings with nucleon transfer channels proved to be certainly important in the near and sub-barrier fusion processes. Nevertheless, their role in fusion reactions is still controversial [11-14]. Recently, an upgrade of the CCQEL [15] code was done by improving the method of coupling to the transfer channels during fusion and backscattering processes [16]. In particular, the number of transfer reactions included has been increased and the dependence of the strength of transfer coupling on the transferred particle and experimental Q -value distributions were introduced. The upgraded code was employed for the investigation of the influence of transfer on the smoothing of the measured D_{qe} of the $^{20}\text{Ne}+^{208}\text{Pb}$ system, for which the Q -value distributions were measured at two projectile's kinetic energies. The study points out that at the higher beam energy, the one-neutron pick-up mainly influences the smoothing of the D_{qe} , while the one-neutron pick-up and one-proton stripping transfers are dominant for the lower beam energy. Such results suggest the need to include a dependence of the transfer coupling on the projectile kinetic energy.

The most direct method to obtain experimental information about the influence of the dissipation due to transfer channels on the D_{qe} is the measurement of the transfer cross-sections. By measuring the transfer cross-sections for various transfer channels and comparing the results for the neighbour isotopes, it is possible to determine whether the transfer couplings might play a significant role in the dynamic of the reaction [17-19]. This can be performed by the direct measurement of the transfer cross-sections at a backward angle, since at energies near the Coulomb barrier the transfer angular distribution has a flat maximum at backward angles. Thus, the measurement performed at one backward angle should give good information about the contributions of the various transfer channels.

An experiment of this kind was performed recently at HIL for the $^{20}\text{Ne}+^{92,94,95}\text{Mo}$ systems. The U200-P Cyclotron of HIL provided the ^{20}Ne beam at an average current of 20 enA and energies of 73 and 71 MeV, while lower energies of 68 and 66 MeV were obtained by employing thin ^{nat}Ni and ^{nat}Au degraders. The four different beam energies were chosen in order to investigate the presence of significant variation in the strength of transfer channels at energies around the Coulomb barrier and that might be related to the barrier distribution's structure [16]. The identification in mass of the products was performed by employing an array of 13 silicon detectors combined with a Microchannel Plate (MCP) detector placed at the backward angle of 142 degrees, while at the same angle, an E - ΔE telescope provided their charge identification. Three silicon detectors at forward angles were used for precise beam energy measurement and monitoring.

Figure 2 shows the E-ToF matrices for the three systems at the beam energy of 73 MeV. Such preliminary results indicate the transfer leading to the mass $A = 19$ and 16 as the main transfer channels in all three systems, but in the case of the ^{95}Mo also one neutron pick-up transfer ($A = 21$) occurred. The analysis is ongoing and should clarify

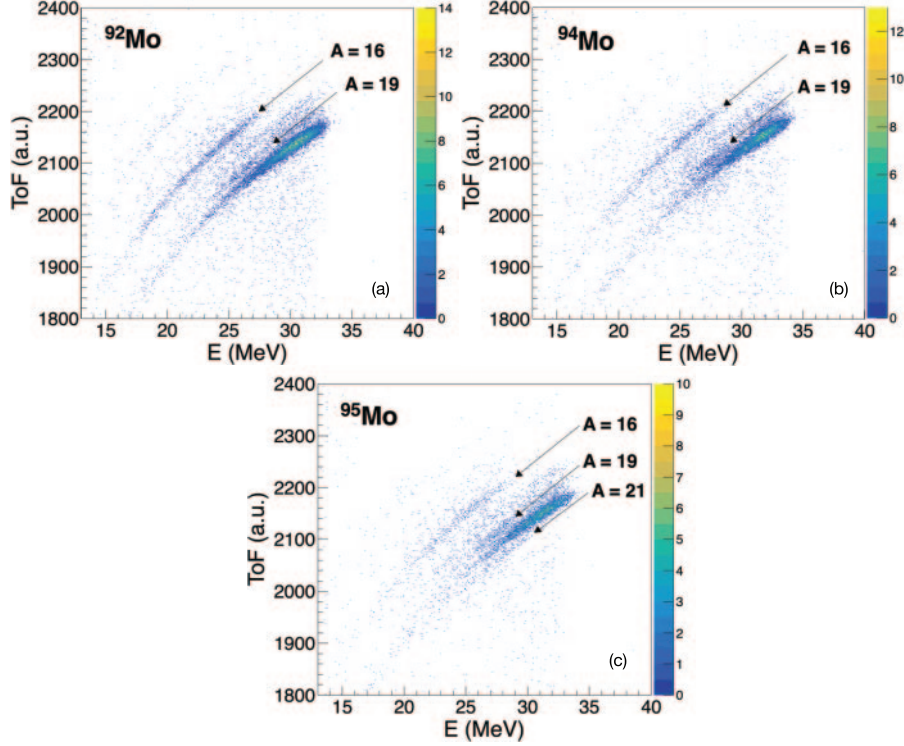


Fig. 2. – Transfer products' identification in mass for $^{20}\text{Ne} + ^{92,94,95}\text{Mo}$ systems at the beam energy of 73 MeV.

the influence that such transfer channels might have on the different structures of the barrier distributions.

4. – Future perspectives

Barrier distribution can be determined directly from the fusion excitation function [2] or the cross-sections of quasielastically back-scattered events [20]. Indeed, the barrier transmission and reflection are complementary to each other, therefore the barrier distributions can be determined by detecting the ions which penetrate or are reflected from the barrier. The main advantage of using the quasielastic representation of the barrier distribution is that it leads to much smaller experimental uncertainties above the Coulomb barrier than the fusion one and it requires much simpler experimental setups for the measurements. On the other hand, the backscattering method might be less sensitive to nuclear structure effects. Up to now only for a few systems, the barrier distribution was extracted with both methods [5, 11, 21], mainly because of the necessity of employing different setups.

In this perspective, at HIL a new setup for fusion cross-section measurement based on a Wien Filter will be installed. The Wien Filter (WiFi), based on the one developed at the Australian National University (ANU) Laboratory [22] has been built and in-beam tested at Laboratori Nazionali del Sud (LNS) [23, 24]. The devices' configuration

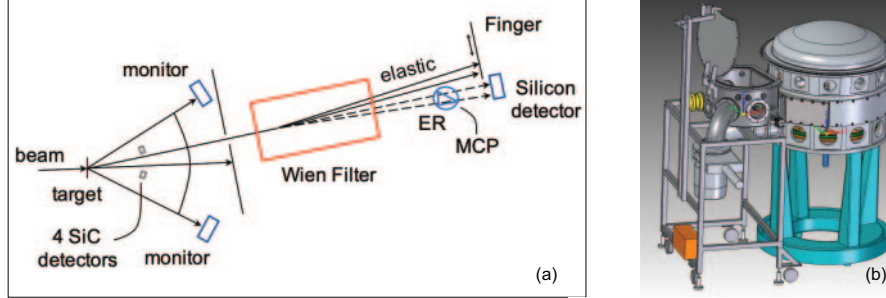


Fig. 3. – (a) Scheme of the experimental setup for near and sub-barrier fusion measurements. (b) AutoCAD drawing of the ICARE scattering chamber and its extension.

is similar to the one employed at the ANU and is shown in fig. 3(a). The identification of the fusion products is performed downstream of the Wien Filter through an MCP and a silicon detector, which will provide the Time of Flight (ToF) and energy of the transmitted particles. A tantalum finger located in front of the silicon detector intercepts the scattered particles and two silicon detectors placed at forward angles are used for precise beam energy measurement.

To perform fusion measurement at HIL, the ICARE scattering chamber has been upgraded with an extension, shown in fig. 3(b), equipped with a moveable platform where the WiFi and a ToF device will be placed. To ensure a more stable beam's position on the target, a beam monitoring system based on four-crossed Silicon Carbide (SiC) detectors will be employed. This beam monitoring system has been successfully tested at HIL [25, 26].

The commissioning of the new setup has been approved by the HIL Programme Advisory Committee and will be performed soon. After the commissioning, the setup will be employed to investigate the role of dissipation due to non-collective excitation on the fusion barrier distributions; a study that so far has been limited to the quasielastic one. Our plan consists in measuring the fusion excitation function and barrier distributions of the $^{20}\text{Ne}+^{92,94,95}\text{Mo}$ systems, and subsequently of other systems of interest.

Finally, the $^{24}\text{Mg}+^{90,92}\text{Zr}$ fusion excitation function will be investigated at the beam energy range of 63–90 MeV, using the Wien Filter and the ToF technique, at LNS Tandem in an experiment to be realized as soon as the LNS accelerators upgrade will be completed [27].

5. – Conclusion and summary

The influence of dissipation due to non-collective excitations on the quasielastic barrier distributions of the $^{20}\text{Ne}+^{92,94,95}\text{Mo}$ systems was studied. The comparison with the CC predictions shows a significant smoothing out of the structure of the barrier distribution for the heavier Mo isotopes, where the level density is larger. The CCRMT calculations obtained including the coupling to s.p. excitations are in good agreement with experimental data, supporting the concept that weak but numerous s.p. excitations can alter the structure of barrier distributions. Surprisingly, the structure of the ^{95}Mo is slightly narrower than that of the ^{94}Mo , despite the lower level density of the latter. Preliminary results of the recently measured differential transfer cross-sections of the

three systems suggest that there might be some differences in the transfer channels of the ^{95}Mo with respect to the $^{92,94}\text{Mo}$ isotopes. However, further studies are necessary to comprehend the role that dissipation due to transfer might have on the structure of the barrier distribution of the $^{20}\text{Ne}+^{92,94,95}\text{Mo}$ systems. A new setup based on a Wien Filter will soon be installed at HIL and should allow extending these studies to fusion excitation functions and barrier distributions.

* * *

This work was funded in part by the SHENG1 project, under contract No. 2018/30/Q/ ST2/00163. This project has received funding from the European Union's Horizon Europe Research and Innovation program under Grant Agreement No 101057511 (EURO-LABS) and by NextGeneration EU project, through MUR-PNRR ecosystem SAMOTHRACE (ECS00000022). The work was also partially supported by the Polish National Science Centre (Grant No. 2020/39/D/ST2/00466).

REFERENCES

- [1] TAMURA T., *Rev. Mod. Phys.*, **37** (1965) 679.
- [2] ROWLEY N., SATCHLER G. R. and STELSON P. H., *Phys. Lett. B*, **254** (1991) 25.
- [3] DASGUPTA M. *et al.*, *Annu. Rev. Nucl. Part. Sci.*, **48** (1998) 401.
- [4] PIASECKI E. *et al.*, *Phys. Rev. C*, **80** (2009) 054613.
- [5] PIASECKI E. *et al.*, *Phys. Rev. C*, **85** (2012) 054608.
- [6] TRZCIŃSKA A. *et al.*, *Phys. Rev. C*, **92** (2015) 034619.
- [7] TRZCIŃSKA A. *et al.*, *Phys. Rev. C*, **102** (2020) 034617.
- [8] YUSA S., HAGINO K. and ROWLEY N., *Phys. Rev. C*, **82** (2010) 024606.
- [9] PIASECKI E. *et al.*, *Phys. Rev. C*, **100** (2019) 014616.
- [10] COLUCCI G. *et al.*, *Acta Phys. Pol. B Suppl.*, **17** (2023) 3-A23.
- [11] TIMMERS H. *et al.*, *Nucl. Phys. A*, **633** (1998) 421.
- [12] BECKERMAN M. *et al.*, *Phys. Rev. Lett*, **45** (1980) 1472.
- [13] BROGLIA R. A. *et al.*, *Phys. Rev. C*, **27** (1983) 2433.
- [14] SCARLASSARA F. *et al.*, *Nucl. Phys. A*, **672** (2000) 99.
- [15] HAGINO K., ROWLEY N. and KRUPPA A. T., *Comput. Phys. Commun.*, **123** (1999) 143.
- [16] COLUCCI G. *et al.*, *Phys. Rev. C*, **109** (2024) 064625.
- [17] PIASECKI E. *et al.*, *Phys. Rev. C*, **85** (2012) 054604.
- [18] TRZCIŃSKA A. *et al.*, *Phys. Rev. C*, **93** (2016) 054604.
- [19] WÓJCIK D. *et al.*, *Acta Phys. Pol. B*, **49** (2018) 387.
- [20] TIMMERS H. *et al.*, *Nucl. Phys. A*, **584** (1995) 190.
- [21] TIMMERS H. *et al.*, *Phys. Lett. B*, **399** (1997) 35.
- [22] WEI J. X. *et al.*, *Nucl. Instrum. Methods A*, **306** (1991).
- [23] PAGANO E. V. *et al.*, *LNS Activity Report 2018/2019* (2018) pp. 57–58.
- [24] PAGANO E. V. *et al.*, *LNS Activity Report 2019* (2019) pp. 51–52.
- [25] PIASECKI E. *et al.*, *HIL Annual Report 2021* (2021) pp. 25–27.
- [26] COLUCCI G. *et al.*, *HIL Annual Report 2022* (2022) pp. 60–62.
- [27] AGODI C. *et al.*, *Eur. Phys. J. Plus*, **138** (2023) 1038.